Asian Journal of Chemistry; Vol. 34, No. 1 (2022), 183-190

ASIAN JOURNAL OF CHEMISTRY

https://doi.org/10.14233/ajchem.2022.23499

Synthesis, Characterization and Antimicrobial Studies of Some New Tellurium(IV) Complexes Derived from 2-[(2-Hydroxyphenyl)imino methyl]-1-naphthol Schiff Base

Mahak Dalal, Manish Kumar, K.K. Verma and Sapana Garg*

Department of Chemistry, Maharshi Dayanand University, Rohtak-124001, India

*Corresponding author: E-mail: sapanagarg1511@gmail.com

Received: 25 August 2021; *Accepted*: 3 October 2021; *Published online*: 16 December 2021; AJC-20634

This article reports the synthesis, characterization and antimicrobial screening of a tridentate 2-[(2-hydroxyphenyl)imino methyl]-1-naphthol ligand (H2AP) and its organotellurium(IV) complexes. Structural characterization of the synthesized ligand and complexes was confirmed by using FT-IR, ^{1}H NMR, ^{13}C NMR, UV-vis, mass spectrometry, molar conductance and elemental analysis. Geometry of all the synthesized compounds has been optimized and their DFT based chemical reactivity descriptors were calculated. DFT and spectral data studies revealed distorted square pyramidal geometry for the tellurium(IV) complexes. *In vitro* antimicrobial activities of the synthesized ligand and its tellurium(IV)complexes were evaluated against two Gram-positive, two Gram-negative bacterial strains and three fungal strains. The tellurium(IV) complexes exhibited promising activity as compared to the Schiff base ligand.

Keywords: Organyltellurium(IV) complexes, DFT study, Antimicrobial activity, Schiff base.

INTRODUCTION

Schiff bases are unsaturated organic molecule characterized by the presence of one or more imine (>C=N-) group [1,2]. These are synthesized from the condensation reaction of aliphatic or aromatic aldehyde/ketones with aliphatic or aromatic amines and are known to show new and unusual structural properties. These properties make the Schiff base ligand exhibits excellent ligand chemistry [3-7]. Over the years, Schiff base ligands have been progressively popular in coordination chemistry due to their flexible coordination modes and multiple metal coordination behaviour. It was found that when Schiff base ligands having a nitrogen, oxygen and sulphur donor atom coordinates with metal ion, the biological activities such as hypoglycemic [8], anticancer [9,10] and DNA cleavage [11,12], antitumour [13,14], antifungal [15], antibacterial [16,17], antiviral [18] and antioxidant [19,20] activities are incredibly enhanced, thus making them extremely useful in medicinal chemistry. Naphthaldehyde derived Schiff bases are among one of the most versatile organic ligands as they have been widely used as catalysts for organic reactions [21-23], precursors for preparation of biological active compounds [24,25] and in the development of efficient electrochemical sensors in the medicare field [26].

Different tellurium(IV) compounds such as tellurium tetrachloride ($TeCl_4$), organotellurium(IV) trichloride ($RTeCl_3$) and diorganotellurium(IV) dichlorides (R_2TeCl_2) are known to act as Lewis acids and form stable complexes [27-29] with oxygen, nitrogen and sulphur donor base including Schiff bases. The tellurium complexes of Schiff base ligands have been found to exhibit a number of biological activities such as antibacterial [30,31], antifungal [32,33], antihelminthic [34] activities, *etc.* Encouraged by the above facts and our interest in the field of tellurium complexes and in continuation of our earlier work on the organotellurium(IV) Schiff base complexes [31,35,36], herein the synthesis, characterization and antimicrobial studies of 2-[(2-hydroxyphenyl)imino methyl]-1-naphthol ligand and its organotellurium(IV) complexes are reported.

EXPERIMENTAL

The chemicals used were purchased from Aldrich Chemical Co., USA and of equivalent grade. Solvents used were acquired from CDH, India and were distilled according to the reported methods [37,38]. All the preparations of tellurium compounds were carried under dry nitrogen condition.

Instrumentation: UV-visible spectra were executed in the wavelength range 200-800 nm using a Shimadzu UV-3600

Plus. The elemental analyses (C, H, N) were executed on a Thermo Finnigan CHNS analyzer. The FT-IR spectra were achieved by polyethylene and KBr discs in the far-IR and mid-IR region on FT-IR spectrophotometer. ^{13}C NMR and ^{1}H NMR spectra were obtained on Bruker Advance III-400 MHz NMR spectrometer using DMSO as deuterated solvent and TMS as reference. Melting point of compounds were determined using capillaries. Molar conductance of compounds were measured on a MICROSIL conductometer. Mass spectra were recorded with SCIEX Triple TOF 5600 Mass Spectrometer.

Synthesis of 2-[(2-hydroxyphenyl)iminomethyl]-1-naphthol Schiff base (H2AP): 2-Hydroxy-1-naphthaldehyde (0.035 g, 20 mmol) and 2-aminophenol (0.022 g, 20 mmol) were dissolved in ethanol separately. Then to the ethanolic solution of 2-hydroxy-1-naphthaldehyde, a solution of 2-aminophenol was added with continuous stirring. The resulting solution was stirred continuously under reflux (60 ºC) condition for 5 h [37] (**Scheme-I**). The product obtained was then filtered off, recrystallized with ethanol and dried at room temperature under vacuum condition.

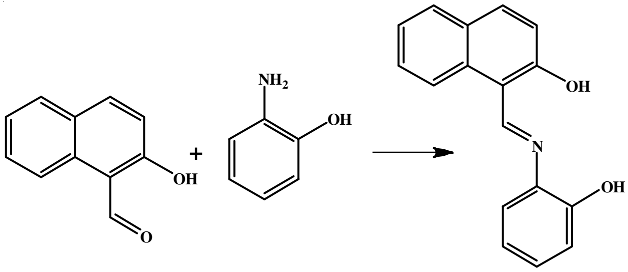

Scheme-I: Synthesis of ligand H2AP

Synthesis of organotellurium(IV) trichlorides ($RTeCl_3$) and diorganotellurium(IV) dichlorides (R_2TeCl_2): Different organotellurium(IV) trichloride ($RTeCl_3$) and diorganotellurium(IV) dichlorides (R_2TeCl_2) were synthesized by the treatment of $TeCl_4$ with methoxybenzene, 2-methylphenol, hydroxybenzene in the molar ratio of 1:1, 1:2 respectively as per the reported procedures [38-48].

$$RH + TeCl_4 \longrightarrow RTeCl_3$$

$$2RH + TeCl_4 \longrightarrow R_2TeCl_2$$

where RH = methoxybenzene, 2-methylphenol and hydroxybenzene.

Synthesis of Schiff base complexes (RTeCl·H2AP and R_2Te·H2AP): These complexes were synthesized by adding different tellurium(IV) derivatives $RTeCl_3$/R_2TeCl_2 (1 mmol in 25 mL methanol) to the solution of ligand H2AP (1 mmol in 25 mL methanol). The solution was refluxed on steam bath at 60 ºC for 4 h under stirring condition. The complexes obtained after slow evaporation of solvent were filtered, recrystallized with methanol and dried under vacuum condition (**Scheme-II**).

Computational calculation: Density functional theory (DFT) calculations were carried out with Orca 4.0 program software. The molecular geometry of ligand and its complexes were fully optimized using DFT based on def2-SVP basis sets. Avogadro 4.0 program package was used for visualization of the optimized structure.

Antimicrobial activity: Schiff base ligand and its organotellurium (IV) complexes (**2a-f**) were assessed for their antimicrobial activity against three fungal strains *viz. A. clavatus* (MTCC 1323), *A. niger* (MTCC 282) and *C. albicans* (MTCC 227); two Gram-negative bacterial strains *viz. E. coli* (MTCC 443), *P. aeruginosa* (MTCC 1688) and two Gram-positive bacterial strains *viz. S. pyogenes* (MTCC 442), *S. aureus* (MTCC 96) by broth dilution method. Minimum inhibitory concentration (MIC) values were calculated by the microdilution technique using concentrations of 1000, 500, 250, 200, 100, 50, 25, 12.5, 6.25 µg/mL. Standard antibiotic ampicillin and greseofulvin were taken as reference.

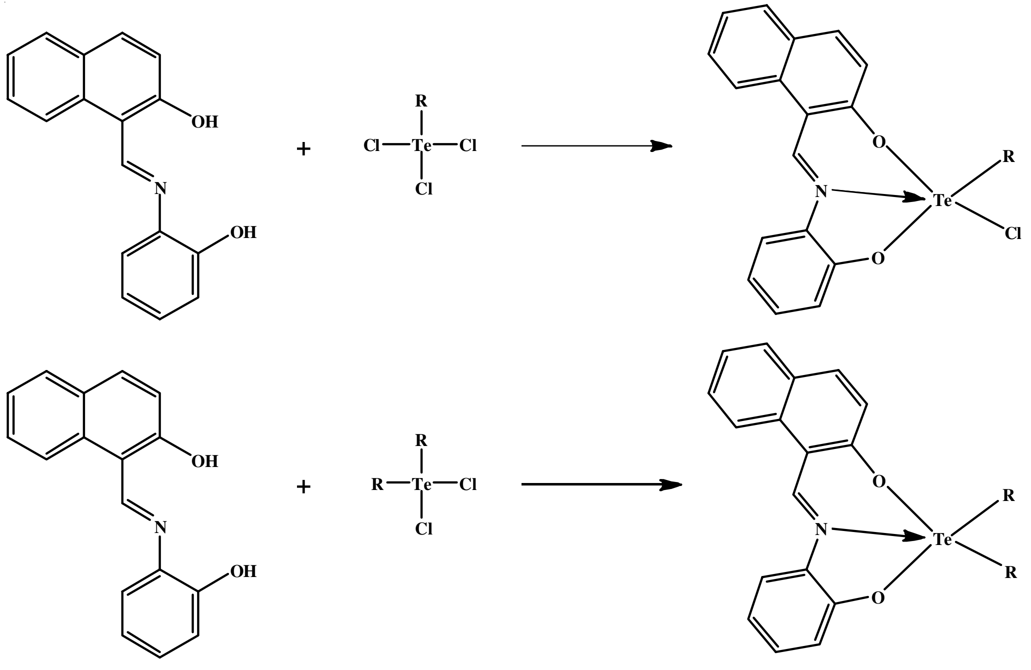

Scheme-II: Synthesis of tellurium metal complexes RTeCl.H2AP and R_2Te.H2AP

TABLE-1
PHYSICAL AND ANALYTICAL DATA OF SCHIFF BASE LIGAND AND ITS ORGANOTELLURIUM(IV) COMPLEXES

Compd. No.	Complex (R)	m.f. (m.w.)	Colour (Yield, %)	m.p. (°C)	Elemental analyses (%): Found (calcd.)				
					C	H	N	Te	Cl
Schiff base	H2AP	$C_{17}H_{13}NO_2$ (263.29)	Dark yellow (76%)	250-254	77.48 (77.55)	5.03 (4.98)	5.29 (5.32)	–	–
2a	RTeCl.H2AP (4-methoxyphenyl)	$C_{24}H_{18}ClNO_3Te$ (531.46)	Dark yellow (73%)	175-179	54.29 (54.24)	3.45 (3.41)	2.59 (2.64)	23.95 (24.01)	6.59 (6.67)
2b	RTeCl.H2AP (4-hydroxyphenyl)	$C_{23}H_{16}ClNO_3Te$ (517.43)	Reddish brown (91%)	190-194	53.44 (53.39)	3.14 (3.10)	2.68 (2.71)	24.62 (24.66)	6.81 (6.87)
2c	RTeCl.H2AP (3-methyl-4-hydroxyphenyl)	$C_{24}H_{18}ClNO_3Te$ (531.46)	Light brown (93%)	191-195	54.20 (54.24)	3.37 (3.41)	2.69 (2.64)	24.00 (24.05)	6.61 (6.67)
2d	R_2Te.H2AP (4-methoxyphenyl)	$C_{31}H_{25}NO_4Te$ (603.13)	Reddish brown (83%)	170-174	61.79 (61.73)	4.13 (4.18)	2.27 (2.32)	21.21 (21.16)	–
2e	R_2Te.H2AP (4-hydroxyphenyl)	$C_{29}H_{21}NO_4Te$ (575.08)	Light brown (80%)	170-174	60.59 (60.57)	3.62 (3.66)	2.50 (2.44)	22.23 (22.19)	–
2f	R_2Te.H2AP (3-methyl-4-hydroxyphenyl)	$C_{31}H_{25}NO_4Te$ (603.13)	Dark green (87%)	110-114	61.68 (61.73)	4.22 (4.18)	2.37 (2.32)	21.22 (21.16)	–

RESULTS AND DISCUSSION

The newly synthesized organotellurium(IV) complexes were coloured, stable at ambient temperature and soluble in organic solvents like DMSO, DMF, *etc*. The physical and analytical data obtained for the ligand (H2AP) and its Te(IV) complexes (**2a-f**) are displayed in Table-1.

Conductance studies: With a view to study the electrolytic nature of the newly synthesized complexes, molar conductance (Λ_M) at ~ 10^{-3}M of complexes were measured in DMSO at 25 ºC. The Λ_M values of complexes lies in the range 36.71-12.35 S cm^2 mol^{-1}, predicting their non-electrolytic nature (Table-2).

TABLE-2
MOLAR CONDUCTANCE DATA OF
ORGANOTELLURIUM(IV) COMPLEXES

Compound	Molar conductance (S cm^2 mol^{-1})
2a	31.12
2b	32.03
2c	36.71
2d	32.54
2e	36.40
2f	12.35

Infrared studies: The characteristic IR frequencies of the Schiff base ligand (H2AP) and its organotellurium(IV) complexes are shown in Table-3. The FT-IR spectra of newly synthesized complexes were analyzed with the spectra of Schiff base to locate coordination sites involved in complexation. The IR spectra of ligand [37,49,50] showed a band at 3440 cm^{-1} due to the stretching vibration of O-H groups present in ligand. This band disappeared on complexation indicating the coordination of tellurium metal through O-H groups after deprotonation. Bonding through oxygen is also supported by the comparative downward shift of C-O frequency in complexes as compared to the ligand. A strong band at 1632 cm^{-1} due to azomethine C=N stretching vibration of ligand [37,49,50], under-goes a shift to lower wavenumber after complexation indicating that nitrogen atom of azomethine is coordinated to tellurium. Also other new bands are observed in the region between 295-285 cm^{-1} and 520-505 cm^{-1} assignable to ν(Te-N) [51,52] and ν(Te-O) [53] stretching vibrations, repectively, supporting the coordination *via* phenolic oxygen, azomethine nitrogen and naphthyl hydroxyl oxygen with tellurium metal.

UV-visible studies: UV-visible spectrum data of Schiff base ligand (H2AP) and its organotellurium(IV) complexes are summarized in Table-4. The electronic absorption spectra of ligand [37,54,55] show four absorption bands, the first two bands at 240 and 303 nm are assignable to π-π* transition associated with the naphthalene unit, shifts to 235 + 20 nm and 300 + 50 nm *i.e.* showing red shift on complexation. The third absorption band at 360 nm is denoted to n-π* electronic transition which shifts to 360 + 50 nm in the complexes. The fourth band at 444 nm is due to the intramolecular charge transfer in the ligand and shifts to 440 + 50 nm in the complexes, suggesting the successful complexation.

TABLE-3
IMPORTANT FT-IR ABSORPTION BANDS (cm^{-1}) OF LIGAND (H2AP) AND ITS ORGANOTELLURIUM(IV) COMPLEXES

Compound	ν(O-H)	ν(C-H) aromatic	ν(C-H) aliphatic	ν(C=N)	ν(C-O)	ν(Te-O)	ν(Te-N)
Ligand	3440m	3020w	2910w	1632s	1265s	–	–
2a	-	3039s	2920 w	1609s	1257s	513s	289s
2b	3154w*	3070w	2911 w	1604s	1256s	517s	289s
2c	3362m*	3062w	2937 w	1605s	1250s	508s	291s
2d	-	3064m	2936 w	1604s	1257s	509s	287s
2e	3420m*	3084w	2940 w	1610s	1254s	519s	295s
2f	3360w*	3153w	2914 w	1625s	1251s	515s	292s

s = sharp, m = medium, b = broad, sh=shoulder and w=weak, *=Due to phenolic OH of RTe and R_2Te moieties.

TABLE-4
UV-VISIBLE ABSORPTION BANDS (λ_{max}) OF SCHIFF BASE (H2AP) AND ITS ORGANOTELLURIUM(IV) COMPLEXES

Compound	π-π* transition, nm (cm^{-1})		n-π* transition, nm (cm^{-1})	Intra ligand transition, nm (cm^{-1})
Ligand	240 (41666)	303 (33003)	360 (27777)	444 (22522)
2a	244 (40983)	305 (32786)	394 (25380)	485 (20618)
2b	248 (40322)	308 (32467)	403 (24814)	480 (20833)
2c	248 (40322)	306 (32679)	385 (25974)	479 (20877)
2d	253 (39525)	308 (32467)	389 (25706)	486 (20576)
2e	247 (40485)	350 (28571)	401 (24937)	489 (20450)
2f	237 (42194)	309 (32362)	387 (25840)	484 (20661)

^{1}H NMR studies: ^{1}H NMR spectrum data of ligand (H2AP) and its complexes are reported in Table-5. In the ^{1}H NMR spectrum, the presence of peak at δ 13.20 ppm and δ 10.86 ppm whose integration corresponds to one proton, is ascribed to the hydrogen bonded naphthyl -OH proton and phenolic proton of aminophenol moiety of ligand [37,54-57]. The absence of such peaks in complexes suggest the participation of both the OH groups in complexation. The singlet peak appeared at δ 8.30 ppm is attributed to azomethine proton and is shifted in the down field region in the complexes suggesting coordination of azomethine nitrogen with tellurium metal. The peaks observed between δ 6.91-8.21 ppm were attributed to aromatic protons of ligand [49] and its organotellurium(IV) complexes.

^{13}C NMR studies: The ^{13}C NMR spectral data of ligand (H2AP) and its complexes are presented in Table-6. In the ^{13}C NMR spectrum, the peaks observed at δ 172.62 ppm, δ 150.00 ppm and δ 147.81 ppm is assigned to azomethine carbon (C_{11}), aromatic carbon attached with -OH group of naphthaldehyde moiety (C_1) and aromatic carbon attached with -OH group of aminophenol moiety (C_{13}) respectively, were found to shifted in the downfield region in the complexes indicating their involvement in complex formation [54,57]. The spectrum of ligand [56] and its organotellurium(IV) complexes also displayed other peaks between δ 106.00-157.60 ppm attributed to the carbons of aromatic rings.

3D Molecular modelling: To understand the molecular structure of ligand (H2AP) and its corresponding complexes, Avogadro 4.0 program with Orca software was used. Full optimization of the ligand (L) and its complexes **2a** and **2e** were carried out without any symmetry constraints. The optimized structures of the Schiff base ligand (H2AP) and the complexes **2a** and **2e** are shown in Fig. 1. Geometrical molecular structure of the Schiff base ligand and complexes were studied after optimization. Optimized values of C-O and C=N bond length (Table-7) for the ligand are 1.350 Å and 1.287 Å which were found to be of 1.364-1.371 Å and 1.291-1.295 Å in complexes indicating their coordination with metal ion. Computed value of the bond angles (Table-8) showed that the tellurium metal in the complexes had a distorted square pyramidal geometry.

TABLE-5
^{1}H NMR SPECTRAL DATA (δ, ppm) OF LIGAND AND ITS ORGANOTELLURIUM(IV) COMPLEXES

Compound	Chemical Shift, δ ppm (in DMSO-d_6)				
	Naphthyl -OH	Phenyl -OH	(CH=N)	Aromatic protons	Aliphatic protons CH_3\OCH_3**
Ligand	13.20 (s, 1H)	10.86 (s, 1H)	8.30 (s, 1H)	6.91-7.98 (m, 10H)	-
2a	-	-	8.92 (s, 1H)	6.91-8.01 (m, 14H)	3.81 (s, 3H)**
2b	-	10.17 (s, 1H)*	9.10 (s, 1H)	6.99-8.09 (m, 14H)	-
2c	-	10.21 (s, 1H)*	9.19 (s, 1H)	6.93-8.21 (m, 13H)	2.10 (s, 3H)
2d	-	-	9.01 (s, 1H)	6.97-8.01 (m, 18H)	3.80 (s, 6H)**
2e	-	10.17 (s, 2H)*	9.10 (s, 1H)	6.98-8.02 (m, 18H)	-
2f	-	10.23 (s, 2H)*	9.21 (s, 1H)	7.01-8.21 (m, 16H)	2.10 (s, 6H)

* = Due to phenolic -OH of RTe and R_2Te moieties, ** = Due to $-OCH_3$ moiety

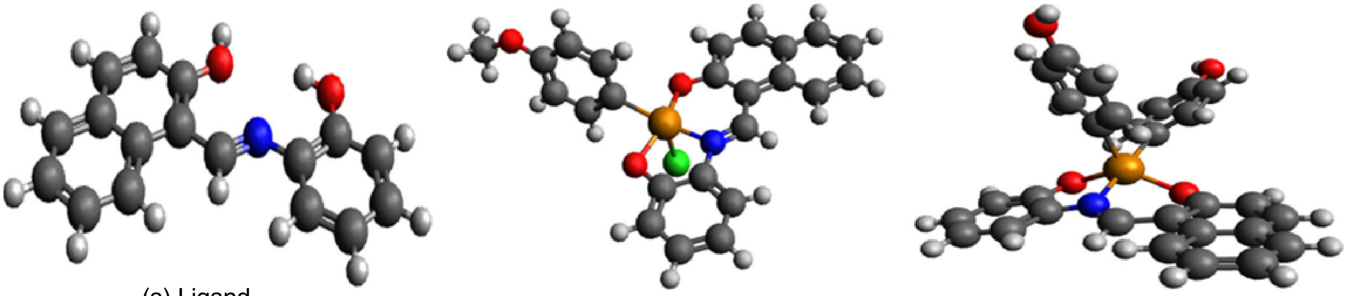

(a) Ligand

(b) Complex **2a**

(c) Complex **2e**

Fig. 1. (a) Optimized structure of ligand H2AP; (b) Optimized structure of complex **2a**; (c) Optimized structure of complex **2e**; Ball colour code: grey-C; red-O; blue-N; green-Cl; yellow-Te; white-H

TABLE-6
^{13}C NMR SPECTRAL DATA (δ, ppm) OF LIGAND AND ITS ORGANOTELLURIUM(IV)COMPLEXES

Compound	Chemical shift, δ ppm (in DMSO-d_6)				
	C=N	C-OH (naphthyl)	C-OH (aminophenol)	Aromatic carbons	Aliphatic carbons (CH_3/OCH_3**)
Ligand	172.62 (C_{11})	150.00 (C_1)	147.81 (C_{13})	118.00 (C_2), 128.40 (C_3), 129.10 (C_4), 126.00 (C_5), 121.90 (C_6), 125.80 (C_7), 117.30 (C_8), 131.00 (C_9), 106.00 (C_{10}), 137.11 (C_{12}), 117.80 (C_{14}), 125.60 (C_{15}), 121.60 (C_{16}), 114.30 (C_{17}).	–
2a	178.35 (C_{11})	154.05 (C_1)	149.91 (C_{13})	118.40 (C_2), 128.70 (C_3), 129.10 (C_4), 126.10 (C_5), 121.90 (C_6), 125.80 (C_7), 117.40 (C_8), 131.00 (C_9), 107.05 (C_{10}), 137.37 (C_{12}), 117.60 (C_{14}), 125.60 (C_{15}), 121.60 (C_{16}), 114.30 (C_{17}), 115.31 (C_{18}), 130.71 ($C_{19,23}$), 123.51 ($C_{20,22}$), 157.60 (C_{21}).	55.30 (C_{24})**
2b	177.67 (C_{11})	154.07 (C_1)	149.97 (C_{13})	118.10 (C_2), 128.50 (C_3), 129.10 (C_4), 126.10 (C_5), 121.90 (C_6), 125.80 (C_7), 117.40 (C_8), 131.03 (C_9), 107.15 (C_{10}), 137.29 (C_{12}), 117.90 (C_{14}), 125.70 (C_{15}), 121.80 (C_{16}), 114.40 (C_{17}), 115.40 (C_{18}), 130.80 ($C_{19,23}$), 117.90 ($C_{20,22}$), 155.01 (C_{21}).	–
2c	176.32 (C_{11})	154.13 (C_1)	151.01 (C_{13})	118.30 (C_2), 128.40 (C_3), 129.10 (C_4), 126.00 (C_5), 121.90 (C_6), 125.80 (C_7), 117.50 (C_8), 131.03 (C_9), 106.50 (C_{10}), 137.97 (C_{12}), 117.80 (C_{14}), 125.70 (C_{15}), 121.80 (C_{16}), 114.40 (C_{17}), 115.40 (C_{18}), 130.80 ($C_{19,23}$), 121.62 (C_{20}), 155.01 (C_{21}), 115.47 (C_{22}).	22.60 (C_{24})
2d	178.31 (C_{11})	154.17 (C_1)	150.11 (C_{13})	118.40 (C_2), 128.70 (C_3), 129.10 (C_4), 126.10 (C_5), 121.90 (C_6), 125.80 (C_7), 117.40 (C_8), 131.00 (C_9), 107.15 (C_{10}), 137.39 (C_{12}), 117.60 (C_{14}), 125.60 (C_{15}), 121.60 (C_{16}), 114.30 (C_{17}), 115.31 ($C_{18,25}$), 130.71 ($C_{19,23,26,30}$), 123.53 ($C_{20,22,27,29}$), 157.60 ($C_{21,28}$).	55.41 ($C_{24,31}$)**
2e	177.69 (C_{11})	154.05 (C_1)	149.99 (C_{13})	118.10 (C_2), 128.50 (C_3), 129.10 (C_4), 126.10 (C_5), 121.90 (C_6), 125.80 (C_7), 117.40 (C_8), 131.03 (C_9), 107.15 (C_{10}), 137.29 (C_{12}), 117.90 (C_{14}), 125.70 (C_{15}), 121.80 (C_{16}), 114.40 (C_{17}), 115.40 ($C_{18,24}$), 130.80 ($C_{19,23,25,29}$), 117.80 ($C_{20,22,26,28}$), 155.03 ($C_{21,27}$).	–
2f	176.30 (C_{11})	154.13 (C_1)	151.11 (C_{13})	118.30 (C_2), 128.40 (C_3), 129.10 (C_4), 126.00 (C_5), 121.90 (C_6), 125.80 (C_7), 117.50 (C_8), 131.03 (C_9), 106.50 (C_{10}), 137.89 (C_{12}), 117.80 (C_{14}), 125.70 (C_{15}), 121.80 (C_{16}), 114.40 (C_{17}), 115.47 ($C_{18.25}$), 130.81 ($C_{19.23.26.30}$), 121.60 ($C_{20.27}$), 155.09 ($C_{21.28}$), 115.49 ($C_{22,29}$).	22.62 ($C_{24,31}$)

** = Due to -OCH_3 moiety

TABLE-7
CALCULATED BOND LENGTH (Å) DATA OF
THE LIGAND H2AP, COMPLEXES **2a** AND **2e**

Compound	C=N	C-O	Te-N (azomethine)	Te-O (phenolic)
Ligand	1.287	1.350	–	–
2a	1.291	1.371	1.901	1.926
2e	1.295	1.364	2.026	1.971

TABLE-8
CALCULATED BOND ANGLES
FOR THE COMPLEX RTeCl.H2AP (**2a**)

Atom connectivity	Bond angles (°)	Atom connectivity	Bond angles (°)
N-Te-O	96.3621	N-Te-O	99.8977
O-Te-Cl	86.2087	N-Te-C	167.0342
O-Te-Cl	84.0173	O-Te-O	159.4775
O-Te-C	83.6984	O-Te-C	83.2415
N-Te-Cl	81.1598	C-Te-Cl	111.7473

Frontier molecular orbital (FMO) analysis: The HOMO/LUMO orbital shapes together with their energy levels are shown in Fig. 2. From the optimized structures, HOMO and LUMO of ligand [56,57] is localized on the entire π-bonding system. In complexes, HOMO is mainly localized on the hetero-atoms surrounding the tellurium metal ion and LUMO is ligand centric with less contribution of tellurium metal ion. Evaluation of HOMO/LUMO energies is beneficial toward estimating about the chemical strength of molecule. The chemical reactivity descriptors such as hardness (η), electrophilicity (ω), chemical potential (Pi), electronegativity (χ), softness (S), additional electronic charge (ΔN_{max}), absolute softness (σ) for the ligand [55] and complexes (**2a** and **2e**) were evaluated from the energy gap (ΔE) between HOMO and LUMO and are illustrated in Table-9. The orbital energy value of HOMO and LUMO of the ligand H2AP were -5.292 eV and -2.991 eV. The ΔE value for the ligand is 2.301 eV. For the complex **2a** and **2e**, the values of HOMO and LUMO energies were at -4.386 eV, -4.235 eV and -2.385 eV, -2.335 eV. The energy gap for complex **2a** and

TABLE-9
THEORETICAL CALCULATED QUANTUM CHEMICAL
PARAMETERS OF LIGAND AND COMPLEXES **2a** AND **2e**

Parameters	Ligand	**2a**	**2e**
E_{HOMO} (eV)	-5.292	-4.386	-4.235
E_{LUMO} (eV)	-2.991	-2.385	-2.335
ΔE (eV)	2.301	2.001	1.900
I (eV)	5.292	4.386	4.235
A (eV)	2.991	2.385	2.335
χ (eV)	4.141	3.385	3.285
η (eV)	1.150	1.000	0.950
σ (eV^{-1})	0.870	1.000	1.050
S (eV^{-1})	0.434	0.500	0.526
ω (eV)	7.460	5.730	5.676
Pi (eV)	-4.141	-3.385	-3.285
ΔN_{max}	3.600	3.385	3.457

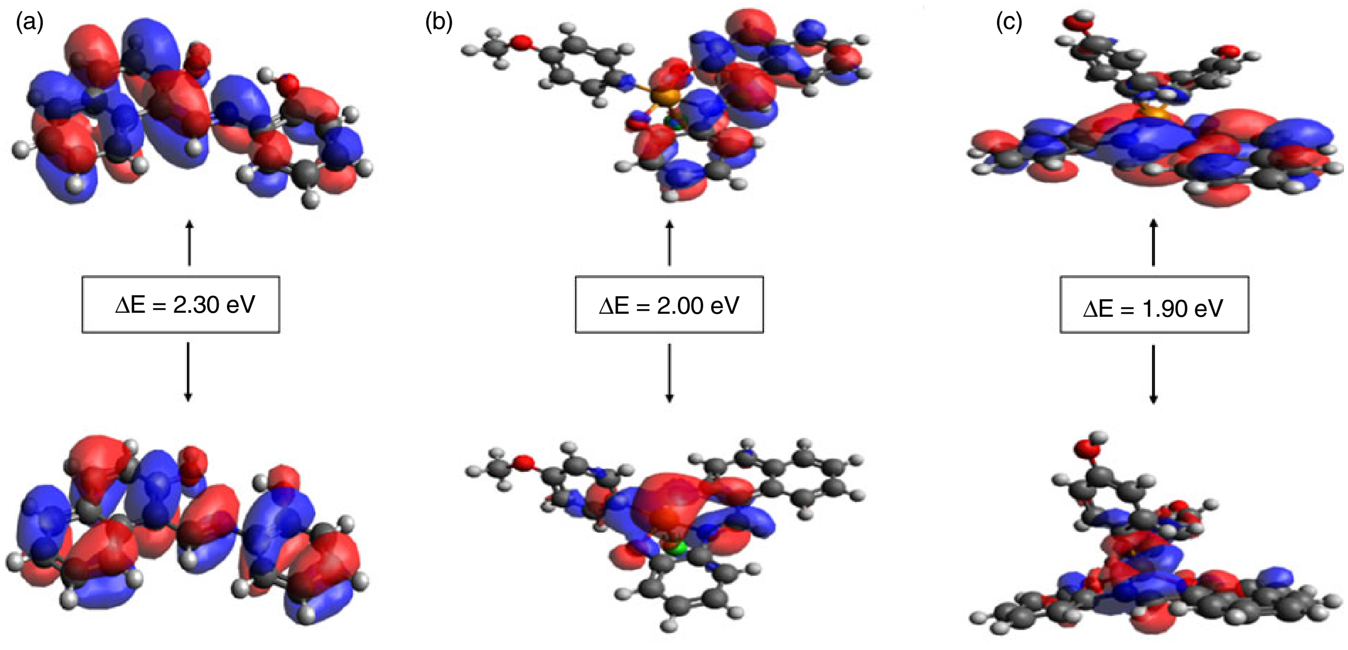

Ligand Complex **2a** Complex **2e**

Fig. 2. (a) HOMO-LUMO gap energies of ligand; (b) HOMO-LUMO gap energies of complex **2a**; (c) HOMO-LUMO gap energies of complex **2e**

2e is 2.001 eV and 1.900 eV, respectively. Subsequent reduction in energy gap observed from ligand to complexes depicts their successful complexation and stability.

Mass studies: The formation of ligand (H2AP) and its organotellurium(IV) complexes were studied with mass spectra. The molecular ion peak for the ligand [54,55,57] H2AP was observed at *m/z* 264.10, which coincides with the calculated molecular mass of Schiff base ligand. For complexes **2a**, **2b**, **2c**, **2d**, **2e** and **2f**, the *m/z* values observed in mass spectrum were at 531.41, 517.39, 531.70, 606.46, 575.08 and 603.13. The data obtained was in good agreement with their proposed molecular formula. The mass spectrum of the ligand H2AP and organotellurium(IV) complex **2d** are shown in Figs. 3 and 4.

Antimicrobial evaluation: The synthesized ligand (H2AP) and its organotellurium(IV) complexes were assessed for their inhibitory effect against few microorganisms using broth dilution method. The minimum inhibitory concentration (mg\mL) were determined using the microdilution method and are reported in Table-10. According to these results, the Schiff base and its organotellurium(IV) complexes represented good antimicrobial activity against all the fungal and bacterial strains. Organotellurium(IV) complexes showed pronounced antimicrobial activity as compared to the Schiff base ligand (H2AP), ascribed to the chelation process occurring in complexes. This pronounced activity can be described by Tweedy theory, according to which chelation process decreases the polarity of metal ion and enhances the lipophilic character of chelate, favouring its penetration through lipid layer of cell membrane thereby blocking metal binding sites for microorganism. Among the synthesized complexes, all were exhibiting potent antibacterial activity against *S. aureus* bacterial strain. Complex **2c** showed highest activity against all the tested bacterial strains, showing

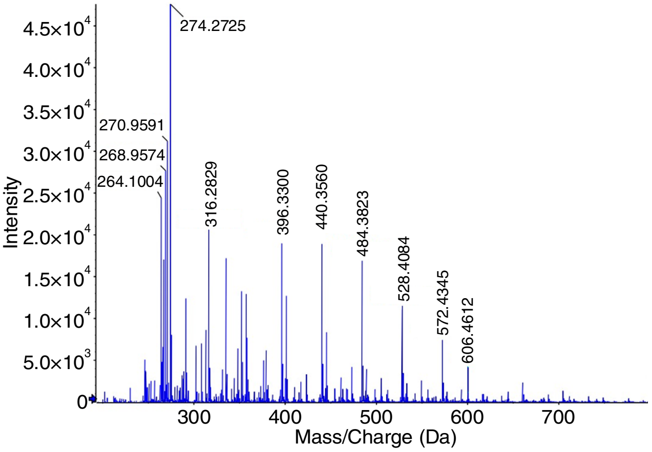

Fig. 4. Mass spectrum of the complex $R_2Te.H2AP$ (**2d**)

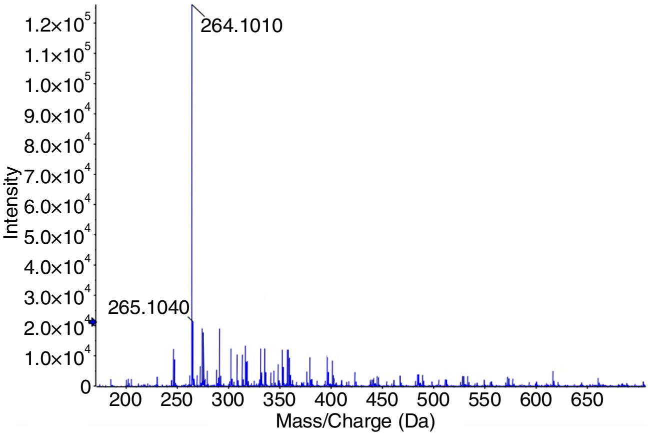

Fig. 3. Mass spectrum of the ligand H2AP

TABLE-10
MINIMUM INHIBITORY CONCENTRATION OF LIGAND (H2AP) AND ITS ORGANOTELLURIUM(IV) COMPLEXES (**2a-f**) AGAINST THE GROWTH OF BACTERIAL AND FUNGAL STRAINS (mg/mL)

Compounds	Bacterial strain				Fungal strain		
	S. aureus	*S. pyogenes*	*E. coli*	*P. aeruginosa*	*C. albicans*	*A. niger*	*A. clavatus*
Ligand	0.25	0.5	0.2	0.125	1.0	1.0	1.0
2a	0.1	0.5	0.25	0.2	0.2	0.1	0.1
2b	0.1	0.25	0.25	0.25	0.5	0.5	1.0
2c	0.0625	0.2	0.125	0.1	0.5	0.5	1.0
2d	0.125	0.2	0.5	0.1	0.25	0.5	0.5
2e	0.2	0.25	0.2	0.5	0.2	0.25	0.25
2f	0.5	0.2	0.25	0.5	0.25	0.5	0.5
Ampicillin	0.25	0.1	0.1	0.1	–	–	–
Greseofulvin	–	–	–	–	0.5	0.1	0.1

lowest MIC value as compared to the standard drug ampicillin. The results of antifungal activity of complexes were compared with the standard drug greseofulvin, it was found that the complexes were highly active against *C. albicans* fungal strain as compared to the fungal strain *A. niger* and *A. clavatus*. Complex **2a** possessed highest antifungal activity against all the fungal strains.

Conclusion

Six organotellurium(IV) complexes (**2a-f**) of ligand (H2AP) have been prepared and characterized through FT-IR, ^{1}H NMR, ^{13}C NMR, UV-vis, mass spectrometry, elemental analyses and conductance measurements. Based on the spectroscopic studies, ligand was found to be of binegative tridentate nature and coordinate to metal ion through naphthyl-O, azomethine-N and aminophenolic-O with distorted square pyramidal geometry for all the tellurium(IV) complexes. The computational studies also support the distorted square pyramidal geometry of the complexes. The proposed structures for the organotellurium(IV) complexes is shown in Fig. 5. The antimicrobial activities of the synthesized ligand and organotellurium(IV) complexes have been assessed against various fungal and bacterial strains. The results indicated that the organotellurium(IV) complexes exhibited enhanced activity in comparision to the ligand.

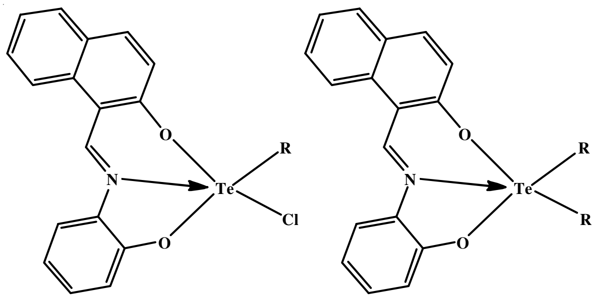

RTeCl.H2AP R$_2$Te.H2AP

Fig. 5. Proposed structure of the organotellurium(IV) complexes

ACKNOWLEDGEMENTS

The authors express their sincere thanks to Maharshi Dayanand University, Rohtak, India for UV and FT-IR analyses. One of the authors, Mahak Dalal thank UGC, New Delhi, India for the financial support. Thanks are also due to Guru Jambheshwar University, Hisar for Mass and NMR spectral analysis, Microcare Laboratory and Tuberculosis Research Centre, Surat for the antimicrobial studies and SAIF, Punjab University for CHN analyses.

CONFLICT OF INTEREST

The authors declare that there is no conflict of interests regarding the publication of this article.

REFERENCES

1. O. Catanescu, M. Grigoras, G. Colotin, A. Dobreanu, N. Hurduc and C.I. Simionescu, *Eur. Polym. J.*, **37**, 2213 (2001); https://doi.org/10.1016/S0014-3057(01)00119-7
2. A. Catalano, M.S. Sinicropi, D. Iacopetta, J. Ceramella, A. Mariconda, C. Rosano, E. Scali, C. Saturnino and P. Longo, *Appl. Sci.*, **11**, 6027 (2021); https://doi.org/10.3390/app11136027
3. S.Q. Memon, M. Memon, A. Mallah, R. Soomro and M.Y. Khuhawar, *Curr. Anal. Chem.*, **10**, 393 (2014); https://doi.org/10.2174/1573411010003140521113731
4. E. Canpolat and M. Kaya, *Russ. J. Coord. Chem.*, **31**, 790 (2005); https://doi.org/10.1007/s11173-005-0170-7
5. I.N. Booysen, S. Maikoo, M. Piers Akerman, B. Xulu and O. Munro, *J. Coord. Chem.*, **66**, 3673 (2013); https://doi.org/10.1080/00958972.2013.849808
6. M. Barwiolek, E. Szlyk, A. Surdykowski and A. Wojtczak, *Dalton Trans.*, **42**, 11476 (2013); https://doi.org/10.1039/c3dt50213a
7. J.M. Fernández-G, F. del Rio-Portilla, B. Quiroz-García, R.A. Toscano and R. Salcedo, *J. Mol. Struct.*, **561**, 197 (2001); https://doi.org/10.1016/S0022-2860(00)00915-7
8. M.A. Mahmoud, A.A. Ammar and S.A. Sallam, *J. Chin. Adv. Mater. Soc.*, **5**, 79 (2017); https://doi.org/10.1080/22243682.2017.1296370
9. G. Gokulnath, P. Anitha, R. Manikandan and C. Umarani, *Asian J. Chem.*, **33**, 1819 (2021); https://doi.org/10.14233/ajchem.2021.23262
10. M.D. Altintop, O. Atli, S. Ilgýn, R. Demirel, A. Özdemir and Z.A. Kaplancikli, *Eur. J. Med. Chem.*, **108**, 406 (2016); https://doi.org/10.1016/j.ejmech.2015.11.041
11. V. Muniyandi and N. Raman, *Mater. Sci. Eng. C*, **68**, 258 (2016); https://doi.org/10.1016/j.msec.2016.05.091
12. A. Charles, R. Krishnaveni and K. Sivaraj, *Asian J. Chem.*, **32**, 3012 (2020); https://doi.org/10.14233/ajchem.2020.22874
13. O.M. Walsh, M.J. Meegan, R.M. Prendergast and T. Al Nakib, *Eur. J. Med. Chem.*, **31**, 989 (1996); https://doi.org/10.1016/S0223-5234(97)86178-8
14. R. Mladenova, M. Ignatova, N. Manolova, T. Petrova and I. Rashkov, *Eur. Polym. J.*, **38**, 989 (2002); https://doi.org/10.1016/S0014-3057(01)00260-9
15. P. Rathelot, N. Azas, H. El-Kashef, F. Delmas, C. Di Giorgio, P. Timon-David, J. Maldonado and P. Vanelle, *Eur. J. Med. Chem.*, **37**, 671 (2002); https://doi.org/10.1016/S0223-5234(02)01388-0

16. G. Kumar, D. Kumar, C.P. Singh, A. Kumar and V.B. Rana, *J. Serb. Chem. Soc.*, **75**, 629 (2010); https://doi.org/10.2298/JSC090704037K
17. M. Tercan, N. Özdemir, F.A. Özdemir, Z. Serbetçi, D. Erdener, B. Çetinkaya and O. Dayan, *J. Mol. Struct.*, **1209**, 127980 (2020); https://doi.org/10.1016/j.molstruc.2020.127980
18. S.P. Chavan and R. Sivappa, *Tetrahedron Lett.*, **45**, 3941 (2004); https://doi.org/10.1016/j.tetlet.2004.03.089
19. M. Sirajuddin, N. Uddin, S. Ali and M.N. Tahir, *Spectrochim. Acta A Mol. Biomol. Spectrosc.*, **116**, 111 (2013); https://doi.org/10.1016/j.saa.2013.06.096
20. R. Selvarani, S. Balasubramaniyan, K. Rajasekar, M. Thairiyaraja and R. Meenakshi, *Asian J. Chem.*, **33**, 1222 (2021); https://doi.org/10.14233/ajchem.2021.23150
21. S.M. Seyedi, R. Sandaroos and G.H. Zohuri, *Chin. Chem. Lett.*, **21**, 1303 (2010); https://doi.org/10.1016/j.cclet.2010.06.009
22. L. Yin, X. Jia, X.S. Li and A.S.C. Chan, *Chin. Chem. Lett.*, **21**, 774 (2010); https://doi.org/10.1016/j.cclet.2010.03.002
23. Y.L. Yang, N.N. Wan, W.P. Wang, Z.F. Xie and J. De Wang, *Chin. Chem. Lett.*, **22**, 1071 (2011); https://doi.org/10.1016/j.cclet.2011.04.014
24. C. Cimarelli and G. Palmieri, *Tetrahedron*, **56**, 475 (2000); https://doi.org/10.1016/S0040-4020(99)01029-7
25. C.P. Singh and H. Hasan, *Asian J. Chem.*, **15**, 49 (2003).
26. M.M. Rahman, T.A. Sheikh, R.M. El-Shishtawy, M.N. Arshad, F.A.M. Al-Zahrani and A.M. Asiri, *RSC Adv.*, **8**, 19754 (2018); https://doi.org/10.1039/C8RA01827H
27. A. Malik, G. Goyat and M. Vikas, *Chem. Sci. Trans.*, **7**, 374 (2018); https://doi.org/10.7598/cst2018.1491
28. A. Malik, G. Goyat and K.K. Vikas, *Chem. Sci. Trans.*, **7**, 329 (2018); https://doi.org/10.7598/cst2018.1480
29. Deepak, K.K. Verma and S. Garg, *Chem. Sci. Trans.*, **6**, 437 (2017); https://doi.org/10.7598/cst2017.1389
30. S. Chhabra and K.K. Verma, *J. Chem. Pharm. Res.*, **2**, 569 (2010).
31. M. Kumar, K.K. Verma and S. Garg, *Asian J. Chem.*, **33**, 1236 (2021); https://doi.org/10.14233/ajchem.2021.23159
32. G. Goyat, S. Garg and K.K. Verma, *Chem. Sci. Trans.*, **5**, 479 (2016); https://doi.org/10.7598/cst2016.1204
33. Deepak, S. Chauhan, K.K. Verma and S. Garg, *Chem. Sci. Trans.*, **6**, 339 (2017); https://doi.org/10.7598/cst2017.1391
34. A.P. Ordyntseva, I.D. Sivovolsva, G.M. Abakarov and E.I. Sadekova, *Pharm. Chem. J.*, **22**, 703 (1988); https://doi.org/10.1007/BF00763667
35. M. Kumar, P.J. Darolia, N. Antil, M. Dalal, J. Narwal, K.K. Verma and S. Garg, *Asian J. Chem.*, **33**, 1749 (2021); https://doi.org/10.14233/ajchem.2021.23214
36. M. Kumar, P.J. Darolia, S. Chauhan, M. Sindhu, K.K. Verma and S. Garg, *ChemistrySelect*, **6**, 5778 (2021); https://doi.org/10.1002/slct.202101184
37. V. Gomathi R.Selvameena R. Subbalakshmi, G. Valarmathy, *Paripex-Ind. J. Res.*, **2**, 11 (2013).
38. A.I. Vogel, Practical Organic Chemistry, Including Qualitative Organic Analysis, Longmans, Green and Co. London, New York, Toranto, Ed. 3, Vol. **1188**, p. 300 (1956).
39. A Weissberger, Technique of Organic Chemistry, Interscience Publishers, Inc.: New York, vol. 7 (1955).
40. B.L. Khandelwal, K. Kumar and F.J. Berry, *Inorg. Chim. Acta*, **47**, 135 (1981); https://doi.org/10.1016/S0020-1693(00)89319-6
41. B.L. Khandelwal, K. Kumar and K. Reina, *Synth. React. Inorg. Met. Chem.*, **11**, 65 (1981); https://doi.org/10.1080/00945718108059276
42. J. Bergman, *Tetrahedron*, **28**, 3323 (1972); https://doi.org/10.1016/S0040-4020(01)93674-9
43. M.V. Garad, *Polyhedron*, **4**, 1353 (1985); https://doi.org/10.1016/S0277-5387(00)86963-6
44. W.J. Geary, *Coord. Chem. Rev.*, **7**, 81 (1971); https://doi.org/10.1016/S0010-8545(00)80009-0
45. F.J. Berry, E.H. Kustan, M. Roshani and B.C. Smith, *J. Organomet. Chem.*, **99**, 115 (1975); https://doi.org/10.1016/S0022-328X(00)86367-6
46. G.T. Morgan and H.D.K. Drew, *J. Chem. Soc. Trans.*, **127**, 2307 (1925); https://doi.org/10.1039/CT9252702307
47. K.K. Verma and K.K. Reena, *Synth. React. Inorg. Met. Chem.*, **29**, 499 (1999); https://doi.org/10.1080/00945719909349465
48. N. Petragnani and H.A. Stefani, Tellurium in Organic Synthesis, Elesevier, Edn. 2 (2007).
49. S. Priyarega, M.M. Tamizh, R. Karvembu, R. Prabhakaran and K. Natarajan, *J. Chem. Sci.*, **123**, 319 (2011); https://doi.org/10.1007/s12039-011-0087-2
50. S. Lirwanu, H. Anas and U. Ziyaulhaq, *Int. J. Adv. Res. Sci. Eng. Tech.*, **5**, 6029 (2018).
51. A. Malik, K.K. Verma and S. Garg, *Chem. Sci. Trans.*, **7**, 191 (2018); https://doi.org/10.7598/cst2018.1464
52. K.K. Verma, D. Soni and S. Verma, *Phosphorus Sulfur Silicon Relat. Elem.*, **166**, 231 (2000); https://doi.org/10.1080/10426500008076544
53. S. Chauhan, S. Garg and K.K. Verma, *Chem. Sci. Trans.*, **5**, 431 (2016); https://doi.org/10.7598/cst2016.1193
54. M.N. Uddin, M.A. Salam, D.A. Chowdhury, J. Sultana and M.E. Halim, *Int. J. Adv. Res. Chem. Sci.*, **1**, 47 (2014).
55. T. Kiran, V.G. Prasanth, M.M. Balamurali, C.S. Vasavi, P. Munusami, K.I. Sathiyanarayanan and M. Pathak, *Inorg. Chim. Acta*, **433**, 26 (2015); https://doi.org/10.1016/j.ica.2015.04.033
56. A.I. Demehin, M.A. Oladipo and B. Semire, *Eclét. Quím.*, **45**, 18 (2020); https://doi.org/10.26850/1678-4618eqj.v45.1.2020.p18-43
57. S. Sarma, A. Bhowmik, M.J. Sarma, S. Banu, P. Phukan and D.K. Das, *Inorg. Chim. Acta*, **469**, 202 (2018); https://doi.org/10.1016/j.ica.2017.09.025